Pergamon

Geochimica et Cosmochimica Acta, Vol. 66, No. 6, pp. 1095–1104, 2002
Copyright © 2002 Elsevier Science Ltd
Printed in the USA. All rights reserved
0016-7037/02 $22.00 + .00

PII S0016-7037(01)00832-8

Kinetic and equilibrium mass-dependent isotope fractionation laws in nature and their geochemical and cosmochemical significance

EDWARD D. YOUNG,[1,*,†] ALBERT GALY,[2] and HIROKO NAGAHARA[3]

[1]Department of Earth Sciences, University of Oxford, Oxford OX1 3PR, UK
[2]Department of Earth Sciences, University of Cambridge, Downing Street, Cambridge CB2 3EQ, UK
[3]Geological Institute, University of Tokyo, Hongo, Tokyo 113, Japan

(*Received March* 30, 2001; *accepted in revised form September* 26, 2001)

Abstract—The mass-dependent fractionation laws that describe the partitioning of isotopes are different for kinetic and equilibrium reactions. These laws are characterized by the exponent relating the fractionation factors for two isotope ratios such that $\alpha_{2/1} = \alpha_{3/1}^{\beta}$. The exponent β for equilibrium exchange is $(1/m_1 - 1/m_2)/(1/m_1 - 1/m_3)$, where m_i are the atomic masses and $m_1 < m_2 < m_3$. For kinetic fractionation, the masses used to evaluate β depend upon the isotopic species in motion. Reduced masses apply for breaking bonds whereas molecular or atomic masses apply for transport processes. In each case the functional form of the kinetic β is $\ln(M_1/M_2)/\ln(M_1/M_3)$, where M_i are the reduced, molecular, or atomic masses. New high-precision Mg isotope ratio data confirm that the distinct equilibrium and kinetic fractionation laws can be resolved for changes in isotope ratios of only 3‰ per amu. The variability in mass-dependent fractionation laws is sufficient to explain the negative $\Delta^{17}O$ of tropospheric O_2 relative to rocks and differences in $\Delta^{17}O$ between carbonate, hydroxyl, and anhydrous silicate in Martian meteorites. (For simplicity, we use integer amu values for masses when evaluating β throughout this paper.) *Copyright © 2002 Elsevier Science Ltd*

1. INTRODUCTION

It is common practice in geochemistry and cosmochemistry to describe mass-dependent isotope fractionation processes with one fractionation law represented by a single curve on a plot of one isotope ratio against another (the three-isotope plot in which isotope ratios are usually expressed as fractional differences from a standard). This practice is justified when the analytical precision associated with light element stable isotope ratio determinations is no better than ± 0.1‰ per amu. It is also common practice to approximate the non-linear fractionation curves as straight lines in three-isotope space. When used to characterize isotope reservoirs on Earth, these straight lines are referred to as terrestrial mass fractionation lines. Deviations from such terrestrial mass fractionation lines are used as indicators of non-mass-dependent isotope effects in geochemistry and cosmochemistry (e.g., Matsuhisa et al., 1978; Luz et al., 1999).

Analytical precision has been improving over the past several years with the result that the assumption of a single fractionation law is no longer valid. Fractionation laws will vary in nature, and in the face of new technologies, it is worth returning to the concepts of mass-dependent fractionation to appreciate the magnitudes and sources of these variations. Most importantly, the existence of different fractionation laws invalidates the concept of a single terrestrial fractionation line for a given isotope system in three-isotope space.

The theoretical basis for mass-dependent isotope fractionation resulting from equilibrium and kinetic processes was established in a series of papers by Bigeleisen, Urey, and others more than 50 yr ago. More recently, Matsuhisa et al. (1978) drew attention to the distinction between equilibrium and kinetic fractionation laws with reference to the three isotopes of oxygen. Nevertheless, because the differences were in the noise of the measurements, the distinction has been largely ignored in subsequent literature.

With the advent of multiple collector-inductively coupled plasma-source mass spectrometry (MC-ICPMS) and improved methods for preparing gases for introduction into gas-source mass spectrometers, there is a new-found ability to measure the relative abundances of the isotopes of O, Mg, Fe, and other elements with precision approaching 50 ppm (e.g., Miller et al., 1999; Galy et al., 2000; Zhu et al., 2001). This new level of precision is sufficient to distinguish different mass fractionation laws over limited ranges in isotopic composition.

Herein we summarize the theoretical basis for mass-dependent isotope fractionation during equilibrium and kinetic processes and explore some of the implications of disparate fractionation laws in geochemistry and cosmochemistry. Mass fractionation laws for equilibrium and kinetic processes differ because kinetic fractionation results from motions that can often be described classically using effective masses whereas equilibrium exchange is purely a quantum phenomenon that depends on the atomic masses alone. The differences between these mass-dependent fractionation laws may explain some effects previously attributed to non-mass-dependent fractionation, and in any case, must be considered when evaluating the significance of apparent departures from a reference mass fractionation line at the sub-per mil level.

2. EQUILIBRIUM MASS-DEPENDENT ISOTOPE FRACTIONATION

Isotope exchange between two compounds can be written as

$$aX_1 + bX_2 = aX_2 + bX_1 \quad (1)$$

* Author to whom correspondence should be addressed (eyoung@ess.ucla.edu).
† *Present address:* Institute of Geophysics and Planetary Physics and Department of Earth & Space Sciences, 595 Charles Young Dr. E., UCLA, Los Angeles, CA 90095, USA.

in which the subscript 2 refers to a heavy isotope and the subscript 1 refers to the light isotope of element X. The equilibrium constant for Eqn. 1 is

$$\mathrm{K_{eq}} = \frac{Q(\mathrm{aX_2})Q(\mathrm{bX_1})}{Q(\mathrm{aX_1})Q(\mathrm{bX_2})} \tag{2}$$

where Q is the partition function for the isotopic species (isotopologue) indicated.

Bigeleisen and Mayer (1947) showed that the partition function ratio for two isotopologues can be written in terms of a classical part and a quantum mechanical part:

$$\frac{Q_2}{Q_1} = f\prod_l \left(\frac{m_{2,l}}{m_{1,l}}\right)^{3/2} \tag{3}$$

where Q_i refers to the partition function of the particular isotopologue i, m_i is the mass of the isotope i, and the product is taken for all isotope atoms l. (In this treatment, symmetry numbers that would otherwise clutter the presentation, but are required when evaluating Eqn. 3 for individual molecules, can be ignored without loss of generality because they cancel in the end results where ratios of partition function ratios are taken. Moments of inertia are also ignored for similar reasons.) The parameter f comprises the quantum part of the partition function ratio for two compounds that differ only in their isotopic composition. The classical term $(m_{2,l}/m_{1,l})^{3/2}$ represents the differences in momentum of the isotopes factored out of the partition function ratio. Although it is central to kinetic fractionation effects, the classical term cancels in balanced reactions where the numbers of each isotope are conserved, and it can be omitted from Q_2/Q_1 when constructing equilibrium constants. For Eqn. 1 the equilibrium constant is then

$$\mathrm{K_{eq}} = \frac{f(\mathrm{aX})}{f(\mathrm{bX})} \tag{4}$$

where f (aX) and f (bX) are the quantum parts of the isotopologue partition function ratios for compounds aX and bX, respectively.

Urey (1947) and Bigeleisen (1955) made use of the fact that f approaches

$$f = 1 + \frac{1}{24}\left(\frac{h}{k_b T}\right)^2 \sum_j (\upsilon_{1,j}^2 - \upsilon_{2,j}^2) \tag{5}$$

to evaluate equilibrium constants at temperatures of several hundred degrees K and higher where quantum effects are small. In Eqn. 5 $\upsilon_{\mathrm{n},j}$ is the frequency of vibration of the n$^{\mathrm{th}}$ isotope, T is temperature, h is Planck's constant, k_b is Boltzmann's constant, and the summation is over all independent vibrational modes j.

Treating the vibrations as harmonic oscillations of the isotopic atoms of interest permits expansion of the differences in the squares of the frequencies of vibration:

$$\upsilon_{1,j}^2 - \upsilon_{2,j}^2 = \frac{K_{f,j}}{4\pi^2}\left(\frac{1}{m_{1,j}} - \frac{1}{m_{2,j}}\right) \tag{6}$$

where $K_{f,j}$ is an appropriate force constant for the atom of interest and vibrational model j. Summing for all vibrations j:

$$\sum_j (\upsilon_{1,j}^2 - \upsilon_{2,j}^2) = \sum_j \left(\frac{1}{m_{1,j}} - \frac{1}{m_{2,j}}\right)\frac{K_{f,j}}{4\pi^2}. \tag{7}$$

Since the masses refer to the atoms in the sum over j, masses can be factored to give for f:

$$f = 1 + \frac{1}{24}\left(\frac{h}{k_b T}\right)^2 \left(\frac{1}{m_1} - \frac{1}{m_2}\right)\sum_j \frac{K_{f,j}}{4\pi^2}. \tag{8}$$

The equilibrium isotope fractionation factor $\alpha^{\mathrm{a-b}}$ for the two substances aX and bX is defined as the ratio of the isotope ratios for these two substances at equilibrium and is equivalent to the equilibrium constant for the exchange reaction:

$$\mathrm{K_{eq}} = \alpha^{\mathrm{a-b}} = \frac{\left(\frac{\mathrm{X_2}}{\mathrm{X_1}}\right)_{\mathrm{a}}}{\left(\frac{\mathrm{X_2}}{\mathrm{X_1}}\right)_{\mathrm{b}}} \tag{9}$$

where each X represents the numbers of isotopes indicated. Eqn. 9, 8, and 4 can be combined to yield expressions for the equilibrium isotope fractionation factor in terms of mass:

$$\ln \alpha^{\mathrm{a-b}} = \ln f_{\mathrm{a}} - \ln f_{\mathrm{b}}. \tag{10}$$

The approximation $\ln(1+\mathrm{x}) \cong x$ can be used to evaluate Eqn. 10 ($f \sim 1.0x$ at 298K), leading to

$$\ln \alpha^{\mathrm{a-b}} = \frac{1}{24}\left(\frac{h}{k_b T}\right)^2 \left(\frac{1}{m_1} - \frac{1}{m_2}\right)\sum_j \left(\frac{K_{f,j,\mathrm{a}}}{4\pi^2} - \frac{K_{f,j,\mathrm{b}}}{4\pi^2}\right) \tag{11}$$

where $K_{f,j,\mathrm{a}}$ and $K_{f,j,\mathrm{b}}$ are the force constants appropriate for atomic species X in compounds a and b, respectively (Weston, 1999).

Eqn. 11 shows that for a given pair of isotopes, the fractionation factor varies from substance to substance according to bond strength. A similar derivation for isotopes 3 and 1 leads to an equation analogous to Eqn. 11. The ratio of the fractionation factors for the two isotope ratios 2/1 and 3/1 is

$$\frac{\ln \alpha_{2/1}^{\mathrm{a-b}}}{\ln \alpha_{3/1}^{\mathrm{a-b}}} = \frac{\frac{1}{24}\left(\frac{h}{k_b T}\right)^2 \left(\frac{1}{m_1} - \frac{1}{m_2}\right)\sum_j \left(\frac{K_{f,j,\mathrm{a}}}{4\pi^2} - \frac{K_{f,j,\mathrm{b}}}{4\pi^2}\right)}{\frac{1}{24}\left(\frac{h}{k_b T}\right)^2 \left(\frac{1}{m_1} - \frac{1}{m_3}\right)\sum_j \left(\frac{K_{f,j,\mathrm{a}}}{4\pi^2} - \frac{K_{f,j,\mathrm{b}}}{4\pi^2}\right)}. \tag{12}$$

This ratio reduces to the mass fractionation law that relates the three isotopes of X at equilibrium

$$\frac{\ln \alpha_{2/1}^{\mathrm{a-b}}}{\ln \alpha_{3/1}^{\mathrm{a-b}}} = \frac{\left(\frac{1}{m_1} - \frac{1}{m_2}\right)}{\left(\frac{1}{m_1} - \frac{1}{m_3}\right)} \tag{13}$$

as shown previously (e.g., Matsuhisa et al., 1978; Weston, 1999). Eqn. 13 can be rearranged to give

$$\alpha_{2/1}^{\mathrm{a-b}} = (\alpha_{3/1}^{\mathrm{a-b}})^{\beta} \tag{14}$$

where

$$\beta = \frac{\left(\frac{1}{m_1} - \frac{1}{m_2}\right)}{\left(\frac{1}{m_1} - \frac{1}{m_3}\right)}. \quad (15)$$

Eqn. 14 and 15 represent a first-order mass-dependent fractionation law for isotope partitioning at equilibrium. They rely on the assertion that the differences in squares of vibrational frequencies in the material depend only on the masses of the isotopes themselves and not on other factors (Eqn. 7). Bigeleisen (1955) discussed the validity of this "rule of the geometric mean" and showed that it holds where mixing is ideal (enthalpies of reaction are zero).

Evaluation of Eqn. 15 gives a unique value for β for a given isotopic system. This is because the masses m_i in Eqn.15 are the atomic masses of the isotopes and not reduced or molecular masses; the equilibrium β value is not sensitive to the masses of the surrounding atoms. For example, Eqn. 6 relies on atomic masses yet there are instances where the frequency of vibration depends on a reduced mass rather than an atomic mass (e.g., diatomic molecules), and on this basis, it might be argued that reduced masses should appear in Eqn. 15. However, it turns out that Eqn. 15 is consistent with the role of reduced masses in determining vibrational frequencies. This is shown by considering a mass M bonded to isotopic species i with masses m_i. The reduced masses are

$$\mu_i = \frac{M\, m_i}{M + m_i}. \quad (16)$$

The difference in the squares of vibrational frequencies for mode j becomes

$$\begin{aligned} \upsilon_{1,j}^2 - \upsilon_{2,j}^2 &= \frac{K_{f,j}}{4\pi^2}\left(\frac{1}{\mu_{1,j}} - \frac{1}{\mu_{2,j}}\right) \\ &= \frac{K_{f,j}}{4\pi^2}\left(\left(\frac{M_j\, m_{1,j}}{M_j + m_{1,j}}\right)^{-1} - \left(\frac{M_j\, m_{2,j}}{M_j + m_{2,j}}\right)^{-1}\right) \\ &= \frac{K_{f,j}}{4\pi^2}\left(\frac{1}{M_j} + \frac{1}{m_{1,j}} - \frac{1}{M_j} - \frac{1}{m_{2,j}}\right) \\ &= \frac{K_{f,j}}{4\pi^2}\left(\frac{1}{m_{1,j}} - \frac{1}{m_{2,j}}\right). \end{aligned} \quad (17)$$

The last line of Eqn. 17 is Eqn. 6. The equivalence of Eqn. 17 and Eqn. 6 shows that the expression for the equilibrium β derived from Eqn. 6 applies regardless of whether or not reduced or atomic masses dictate the vibrational frequencies (we will show that this is not true for the kinetic expression for β). The reader may verify that substitution of reduced masses into Eqn. 15 gives the same values for β as the atomic masses. Molecular masses would not be used to evaluate Eqn. 15 because in the general case, the vibrations are interatomic.

3. KINETIC MASS-DEPENDENT ISOTOPE FRACTIONATION

Equilibrium partitioning of isotopes between compounds depends upon zero-point energy differences that reflect the net effect of numerous vibrational modes. These differences do not arise in the limit of classical mechanics. Kinetic fractionation, on the other hand, can result from motions that are described satisfactorily by classical mechanics. A generalized functional form for the kinetic mass-dependent fractionation law can be derived from the classical part of the partition function ratio in Eqn. 3. However, before describing such a law, it is useful to illustrate the way that kinetic fractionation differs from equilibrium fractionation using a simple example.

If molecules comprising a gas do not interact apart from collisions, then their kinetic energies are the same (treating the gas as ideal). In this case we can calculate the mass fractionation law for three isotopes comprising isotopologues of these molecules. Imagine, for example, collecting the molecules based on their relative velocities. The numbers of isotopic molecules collected will be proportional to the velocities and the velocities a function of mass, such that

$$KE = \frac{1}{2} m_1 \nu_1^2 = \frac{1}{2} m_2 \nu_2^2 = \frac{1}{2} m_3 \nu_3^2 \quad (18)$$

where subscripts 1, 2, and 3 designate the three isotopes (in ascending order of mass), KE is the kinetic energy of the molecules, m is the mass of the indicated isotopologue, and ν is the velocity of the isotopologue. The isotope fractionation factor α can be equated with the ratio of the velocities of the molecules relative to a condition in which the velocities are equal, leading to

$$\frac{\ln \alpha_{2/1}}{\ln \alpha_{3/1}} = \frac{\ln\left(\frac{\nu_2}{\nu_1}\right)}{\ln\left(\frac{\nu_3}{\nu_1}\right)} = \frac{\ln\left(\frac{m_1}{m_2}\right)}{\ln\left(\frac{m_1}{m_3}\right)}. \quad (19)$$

Eqn. 19 shows that the mass fractionation law in this circumstance is

$$\alpha_{2/1} = \alpha_{3/1}^{\beta} \quad (20)$$

where the exponent β is

$$\beta = \frac{\ln\left(\frac{m_1}{m_2}\right)}{\ln\left(\frac{m_1}{m_3}\right)}. \quad (21)$$

Eqn. 21 is evaluated using the molecular masses. The exponent β in this kinetic process is different from that derived for equilibrium isotope partitioning (cf. Eqn. 15). Although we have used approximations to simplify the mathematics, there is nothing inherent in the physics behind the derivations of Eqn. 21 and Eqn. 15 that would require convergence of the two distinct values for β. The distinction is underscored by the realization that Eqn. 21 is a ratio of logarithms of classical partition function ratios ($(m_{2,I}/m_{1,I})^{3/2}$ in Eqn. 3)) for the reactants whereas Eqn. 15 is a ratio of differences in logarithms of partition function ratios (f values in Eqn. 3) between products *and* reactants that would not exist in the classical limit. In brief, exponents for kinetic and equilibrium fractionation laws derive from the mass dependence of different aspects of partition functions.

For more general applicability, a mass fractionation law attending kinetic isotopic exchange can be derived using tran-

sition state theory as shown by Bigeleisen (1949). In this formulation the ratio of rate constants for an elementary reaction proceeding with two different isotope reactants is

$$\frac{k_{f,2}}{k_{f,1}} = \frac{\upsilon_2^*}{\upsilon_1^*}\frac{f_{2/1}^+}{f_{2/1}^{\text{react}}} \tag{22}$$

where $k_{f,2}$ and $k_{f,1}$ are the forward rate constants for two otherwise identical reactions involving isotope 2 and 1 as reactants, respectively, υ_2^* and υ_1^* are frequencies of vibration for the two isotopes in a bond that, when ruptured, leads to formation of the activated complex (transition state), and $f_{2/1}^+/f_{2/1}^{\text{react}}$ is the equilibrium constant for the formation of the transition state from reactants (evaluation of $f_{2/1}^+$ excludes the vibration that becomes the ruptured bond, or reaction coordinate). The ratio of reaction rate constants can be equated with the isotope fractionation factor for a pair of isotopes, that is, $\alpha_{2/1} = k_{f,2}/k_{f,1}$. For harmonic oscillations along what will become the reaction coordinate (allowing the substitution $\upsilon_i^* = 1/(2\pi)\sqrt{K_f/m_i^*}$), the ratio of fractionation factors is

$$\frac{\ln \alpha_{2/1}}{\ln \alpha_{3/1}} = \frac{\frac{1}{2}\ln\left(\frac{m_1^*}{m_2^*}\right) + \ln f_{2/1}^+ - \ln f_{2/1}^{\text{react}}}{\frac{1}{2}\ln\left(\frac{m_1^*}{m_3^*}\right) + \ln f_{3/1}^+ - \ln f_{3/1}^{\text{react}}}. \tag{23}$$

Because $\ln(m_1^*/m_2^*) \gg \ln f_{2/1}^+ - \ln f_{2/1}^{\text{react}}$ and likewise for isotope ratio 3/1, to a good approximation, Eqn. 21 gives the following fractionation law

$$\alpha_{2/1} = (\alpha_{3/1})^\beta \tag{24}$$

where

$$\beta = \frac{\ln\left(\frac{m_1^*}{m_2^*}\right)}{\ln\left(\frac{m_1^*}{m_3^*}\right)}. \tag{25}$$

The masses in Eqn. 25 need not be the atomic masses and could instead refer to, for example, reduced masses of a vibrating diatomic molecule. The kinetic β can therefore vary as a function of the masses of the species bonded to the isotopes of interest.

To explore further the applicability of Eqn. 25, one can derive its equivalent in the context of a quantum mechanical, as opposed to a classical, formulation of transition state theory. The RRKM (Rice-Ramsperger-Kassel-Marcus) theory for unimolecular dissociation can be used for this purpose (Marcus and Rice, 1951).

Start by assuming that the rate constant is determined by the frequency of vibration of a single bond that will become the reaction coordinate in the reactant molecule (the frequency of attempts to break the bond):

$$k_f = \upsilon^*. \tag{26}$$

At the microscopic scale this one frequency of vibration is related to discrete energy levels:

$$E - E_{zp} = \Delta E = nh\upsilon^* \tag{27}$$

where E is the energy associated with vibrational quantum number n, h is Planck's constant, and E_{zp} is the zero-point energy ($1/2h\upsilon^*$). As a result, the forward rate constant for unimolecular dissociation as a function of E is:

$$k_f(E) = \frac{\Delta E}{h}. \tag{28}$$

Eqn. 26 and 28 are manifestations of the usual "smearing" of energy at a given frequency as prescribed by the uncertainty principle (Forst, 1973). Generally, more than one vibrational mode can contribute to formation of the transition state and bond rupture, because anharmonic vibrations can couple. In this case the ΔE in Eqn. 28 must be evaluated from the density of states at E. The rate constant becomes

$$k_f(E) = \frac{1}{h\rho(E)} \tag{29}$$

where $\rho(E)$ is the density of states for energy E for the reactant molecule (J^{-1}). In addition, Eqn. 29 may apply to more than one quantum state accessible to the activated complex. The number of these states is designated as N^+. The complete equation for the forward rate constant becomes

$$k_f(E) = \frac{N^+}{h\rho(E)}. \tag{30}$$

For a single vibration contributing to bond rupture, $\rho(E) = dn/dE = 1/(h\upsilon^*)$, and for a single state for the activated complex, the equation for the rate constant reduces to Eqn. 26 (i.e., $k_f(E) = \upsilon^*$). The ratio of rate constants for two isotopologue reactants 1 and 2 is then $\upsilon_2^*/\upsilon_1^*$ which clearly leads to the expression for β in Eqn. 25 as long as the isotopic substitution does not affect the number of quantum states accessible to the transition state (i.e., the usual case; cf. Gao and Marcus, 2001).

For the more general case of multiple vibrations, s in number, Marcus and Rice (1951) showed that the density of states can be calculated as

$$\rho(E) = \frac{(E + E_{zp})^{s-1}}{(s-1)!\prod_{j=1}^{s} h\upsilon_j} \tag{31}$$

where the zero-point energy represents the sum over all vibrations s. The rate constant is then

$$k_f(E) = \frac{N^+}{h}(E + E_{zp})^{1-s}(s-1)!\prod_{j=1}^{s} h\upsilon_j. \tag{32}$$

The ratio of two rate constants for two different isotopic variants of the same reactant molecule gives

$$\ln \alpha_{2/1} = \sum_{j=1}^{s} \ln\left(\frac{\upsilon_{2,j}^*}{\upsilon_{1,j}^*}\right) + (1-s)\ln\left(\frac{E + E_{zp,2}}{E + E_{zp,1}}\right). \tag{33}$$

The ratio of fractionation factors for three isotopologues is

$$\beta \sim \frac{\sum_{j=1}^{s} \ln\left(\frac{\mu_{1,j}}{\mu_{2,j}}\right) + (1 - s)\ln\left(\frac{E_{zp,2}}{E_{zp,1}}\right)}{\sum_{j=1}^{s} \ln\left(\frac{\mu_{1,j}}{\mu_{3,j}}\right) + (1 - s)\ln\left(\frac{E_{zp,3}}{E_{zp,1}}\right)} \quad (34)$$

where we have substituted the expression for the frequency of harmonic oscillators in terms of reduced masses for each vibration s and a truncated Taylor series expansion for the second term on the right-hand side of Eqn. 33. Eqn. 34 reduces to Eqn. 25 when the reduced masses are the same for each vibration contributing to bond rupture. Eqn. 34 leads to β values that are either close to the values obtained from Eqn. 25 or somewhere between the values given by Eqn. 15 and 25; the kinetic β values from Eqn. 34 are usually less than the equilibrium values.

The expression for β in Eqn. 34 characterizes mass-dependent isotope fractionation for a simple unimolecular dissociation as long as the quantum states accessible to the transition state are independent of the isotopic substitutions. If so, then the N^+ terms cancel in going from Eqn. 32 to Eqn. 33. In addition, the density of states for the reactant molecules must reflect intramolecular equilibrium (i.e., the vibrational states at a specified total energy E are all occupied equally) so that the summations in Eqn. 34 apply to each isotopologue. Recently, Hathorn and Marcus (1999, 2000) and Gao and Marcus (2001) have shown that departures from both of these restrictions can explain the mass-independent (or "strange" mass-dependent) fractionation laws that characterize the formation of ozone. These departures from Eqn. 34 are likely to be restricted to certain reactions in the gas phase since nonequilibrium values for $\rho(E)$ rely on short-lived transition states (with life times shorter than the time required for intramolecular equilibration), and both departures are related to the symmetry of the isotopomers (Gao and Marcus, 2001).

Comparing Eqn. 21, 25, and 34 shows that in general, the exponent that characterizes the mass-dependent fractionation law applicable to kinetic processes depends on the motions that determine the rates of a given process. The species in motion may be molecules, atoms, or pairs of atoms, and the masses used to evaluate the kinetic β are assigned accordingly. The motions can be identified with the preexponential term in an Arrhenius reaction rate equation (Slater, 1948). There is no physical reason for β in these rate equations to be identical to the equilibrium β and in general, the kinetic value for β is less than the equilibrium value. We expect Eqn. 25 to be most applicable to reactions involving condensed phases (e.g., evaporation), whereas Eqn. 34 may be required for reactions confined to the gas phase.

4. MASS-FRACTIONATION CURVES IN THREE-ISOTOPE SPACE

In each of the cases examined above the equation that relates the isotope fractionation factors for three isotopes is of the form

$$\alpha_{2/1} = \alpha_{3/1}^{\beta} \quad (35)$$

where the functional dependence of β varies depending upon the process. The formula for any fractionation curve in which one isotope ratio is plotted against the other is

$$^{2/1}R = {}^{3/1}R^{\beta}\ (^{2/1}R_{ref}/{}^{3/1}R_{ref}^{\beta}) \quad (36)$$

where $^{2/1}R$ and $^{3/1}R$ are the 2/1 and 3/1 isotope ratios for each datum on the curve and $^{2/1}R_{ref}$ and $^{3/1}R_{ref}$ are the isotope ratios for a reference material on the curve. The fractionation curves can be rewritten in terms of the standard delta notation where $\delta^{i/1} = (^{i/1}R/{}^{i/1}R_{std} - 1)\ 10^3$ and $^{i/1}R_{std}$ is the isotope ratio of a standard material (e.g., Standard Mean Ocean Water, or SMOW, in oxygen isotope work):

$$\delta^{2/1} = (10^3 + \delta_{ref}^{2/1})\left(\frac{10^3 + \delta^{3/1}}{10^3 + \delta_{ref}^{3/1}}\right)^{\beta} - 10^3. \quad (37)$$

Eqn. 37 is the equation for a fractionation curve in a plot of $\delta^{2/1}$ (ordinate) against $\delta^{3/1}$ (abscissa), the usual form of the three-isotope plot. In this equation the reference composition lies on the curve and all of the δ values are relative to the same standard (the standard need not be on the same fractionation curve as the reference in this equation). The resulting fractionation curves are non-linear.

5. EXTRACTING THE FRACTIONATION EXPONENT FROM DATA

Hulston and Thode (1965) showed that the relationship between $\delta^{2/1}$ and $\delta^{3/1}$ in Eqn. 37 can be linearlized if the definitions of the δ values are redefined such that $\delta'^{i/1} = 10^3 \ln(^{i/1}R/{}^{i/1}R_{std})$. Miller et al. (1999) used the Hulston and Thode (1965) definition of δ to determine a precise value for the mass fractionation exponent β that best characterizes oxygen isotope fractionation among rocks from a wide range of geologic environments.

In the Hulston and Thode (1965) definition of δ, referred to hereafter as δ', $\ln(^{i/1}R/{}^{i/1}R_{std})$ replaces $(^{i/1}R/{}^{i/1}R_{std} - 1)$. These two quantities are the same where $^{i/1}R/{}^{i/1}R_{std} = 1$ but diverge at all other values for which both are defined. The mass fractionation curves in terms of δ' are straight lines of the form

$$\delta'^{2/1} = \beta\ \delta'^{3/1} - \beta\ \delta'^{3/1}_{ref} - \delta'^{2/1}_{ref} \quad (38)$$

where the reference composition (ref) is any point on the mass fractionation curve, whereas the standard used to define the δ' values (e.g., SMOW) need not be on the curve. Eqn. 38 can be used to extract the exponent β that characterizes a fractionation law by linear regression of a set of isotope ratio data expressed in terms of δ'. This is the approach used by Miller et al. (1999).

6. APPLICATIONS

6.1. Mg Isotope Fractionation During Evaporation

Evaporation may have influenced the elemental and isotopic variability among some early solar system materials. Experiments in which primitive solar system rocks are evaporated or sublimed at low pressures in the laboratory serve as means for evaluating the effects of total pressures and partial pressures (e.g., pressure of H_2) on the evaporation process. Analyses of $^{25}Mg/^{24}Mg$ and $^{26}Mg/^{24}Mg$ from evaporative residues produced by this type of experiment at the University of Tokyo provide the opportunity to test the prediction that evaporation,

a kinetic process, will result in a fractionation law with $\beta \sim \ln(m_1/m_2)/\ln(m_1/m_3)$.

6.1.1. Experimental methods

In these experiments chondrules were evaporated in a high-temperature furnace within a vacuum chamber (Nagahara and Ozawa, 1996). The heater was tungsten mesh with a diameter of 5 cm and a height of 10 cm. Individual chondrules from the Bjurbole and Allende chondrite meteorites were placed on a molybdenum screen set in the center of the furnace assembly. The samples were heated from room temperature to 773K in 20 min and held at that temperature until pressures of $< 1 \times 10^{-10}$ bar were achieved (requiring several hours). The chondrules were then partially evaporated at pressures ranging from 10^{-10} to 10^{-6} bar at a temperature of 1773K. The higher steady-state pressure was achieved by bleeding H_2 into the chamber during evaporation. Temperature was controlled with a W95Re5-W74Re26 thermocouple calibrated against the melting temperatures of Fe, Ni, and Pt. Following heating, the samples were cooled by turning off the heater (a subsolidus temperature of 1273K was achieved in $<$ 2 min).

The $^{25}Mg/^{24}Mg$ and $^{26}Mg/^{24}Mg$ analyses were obtained by MC-ICPMS, following acid digestion of the residues and starting materials and purification of the extracted Mg as described by Galy et al. (2000, 2001). All samples were digested in distilled HF and HNO_3. The Mg in solution was purified by removing Fe and Al as precipitates and Ca and Na by cation exchange (Dowex AG50W-X12). Purification eliminates matrix effects and isobaric interferences arising from coexisting elements in the samples (e.g., $^{48}Ca^{++}$, NaH^+). The weak nitric acid solutions containing the isolated Mg were introduced into the plasma source of the mass spectrometer through a modified Cetac MCN 6000 desolvating nebulizer. The desolvating nebulizer limits isobaric interferences from extraneous oxides, carbides, and nitrides to negligible levels (e.g., $C_2H_2^+$, CN^+). Magnesium isotope ratios were measured using a Nu Instruments MC-ICPMS. This double-focusing instrument has variable-dispersion ion optics and a fixed array of 12 Faraday collectors. The working mass resolution for flattop peaks is ~300. The isotope ratios $^{25}Mg/^{24}Mg$ and $^{26}Mg/^{24}Mg$ are reported relative to the SRM 980 international Mg standard (Catanzaro et al., 1966) as $\delta^{25}Mg = ((^{25}Mg/^{24}Mg)_{sample}/(^{25}Mg/^{24}Mg)_{SRM\ 980} - 1)10^3$ and $\delta^{26}Mg = ((^{26}Mg/^{24}Mg)_{sample}/(^{26}Mg/^{24}Mg)_{SRM\ 980} - 1)10^3$. The long-term reproducibility of the method is $\pm$ 0.03‰ 1σ for $\delta^{25}Mg$ and $\pm$ 0.06‰ 1σ for $\delta^{26}Mg$ (Galy et al., 2000, 2001). The correlation coefficient between measured $\delta^{25}Mg$ and $\delta^{26}Mg$ values is 0.793 (represented by the orientation of the error ellipses in Figure 1.

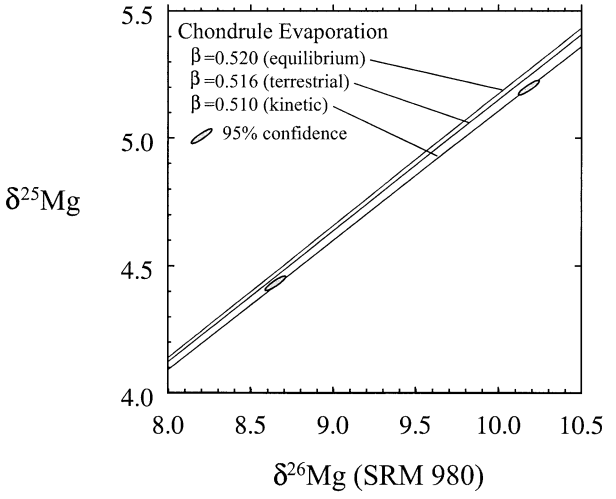

Fig. 1. Magnesium three-isotope plot of residues from evaporation of chondrules (only the most fractionated samples are shown at this scale) showing that different fractionation laws can be distinguished with the uncertainties associated with the data. The 95% confidence level error ellipses represent the eigenvectors and eigenvalues (multiplied by the χ-squared factor to achieve the 95% confidence level) for the covariance matrix obtained from the long-term reproducibility of the method ($\pm$ 0.03‰ 1σ for $\delta^{25}Mg$ and $\pm$ 0.06‰ 1σ for $\delta^{26}Mg$, as reported by Galy et al., 2000, 2001; and the correlation coefficient of 0.793 obtained from $\delta^{25}Mg$ and $\delta^{26}Mg$, standard data). The three fractionation curves are centered at $\delta^{25}Mg$ = 1.66‰ and $\delta^{26}Mg$ = 3.42‰ on the SRM 980 scale. Note that the data define a fractionation curve indistinguishable from the kinetic fractionation law.

6.1.2. Results

Eqn. 25 predicts that the mass fractionation curve on a plot of $\delta^{25}Mg$ against $\delta^{26}Mg$ (both relative to the SRM 980 standard) will be characterized by $\beta = 0.5100$ for a kinetic process like evaporation (Mg is well known to evaporate as the monatomic species). Linear regression of the evaporation residue

Table 1. Results of chondrule evaporation experiments on four chondrules from the Allende and Bjurbole meteorites.

Sample	Type†	Pressure (bar)	Temp. (K)	$\delta^{26}Mg$‡	$\delta^{25}Mg$‡	$\delta'^{26}Mg$§	$\delta'^{25}Mg$§
Allende 3	I	*	*	3.22	1.66	3.22	1.66
Allende 3	R	4×10^{-6}	1773	10.18	5.20	10.13	5.19
Bjurbole 1	I	*	*	3.22	1.66	3.22	1.66
Bjurbole 1	R	9×10^{-10}	1773	4.28	2.21	4.27	2.20
Bjurbole 3	I	*	*	3.14	1.60	3.14	1.60
Bjurbole 3	R	2×10^{-10}	1773	8.65	4.43	8.61	4.42
Bjurbole 4	I	*	*	2.70	1.41	2.70	1.40
Bjurbole 4	R	4×10^{-6}	1773	4.32	2.22	4.31	2.22

† I = initial material, R = evaporation residue.

‡ $\delta^{25}Mg = ((^{25}Mg/^{24}Mg)_{sample}/(^{25}Mg/^{24}Mg)_{SRM\ 980} - I)10^3$ where SRM 980 is the international Mg standard described by Catanzaro et al. (1966). A similar definition applies to $\delta^{26}Mg$.

§ $\delta'^{25}Mg = 10^3 \ln((^{25}Mg/^{24}Mg)_{sample}/(^{25}Mg/^{24}Mg)_{SRM\ 980})$ as suggested by Hulston and Thode (1965). A similar definition applies to $\delta'^{26}Mg$.

data (Table 1) expressed in terms of the δ' values proposed by Hulston and Thode (1965) yields $\beta = 0.5108 \pm 0.003$ (2σ regressed using the method described by York, 1969). For comparison, the equilibrium value for β based on Eqn. 15 is 0.5200 for monatomic Mg. The difference between the exponents is easily resolvable with the quality of data represented by the evaporation experiments (Fig. 1), and the agreement between the best-fit value for β and that predicted for a kinetic process is taken as validation of the prediction method.

The evaporation data can be compared with the "terrestrial" fractionation curve obtained by analysis of a mixture of terrestrial samples (Fig. 1). Galy et al. (2000, 2001) analyzed 61 terrestrial samples containing Mg with a δ^{25}Mg range of 5.3‰. Regression of the linear form of the isotope data (δ' values) yields $\beta = 0.5163 \pm 0.001$ (2σ, method of York, 1969). The samples analyzed by Galy et al. (2000, 2001) represent a wide range of geologic environments, including several that are likely to reflect kinetic fractionation (e.g., spinach chlorophyll) and others that likely reflect equilibrium fractionation (e.g., metamorphic magnesite). The data of Galy et al. (2000) also include analytical-grade Mg solutions and high-purity Mg metal that define a β of 0.5132 ± 0.0008 (2σ) over a range in δ^{25}Mg values of 2‰, suggesting that chemical purification of Mg resulted in a strong kinetic component to the isotope fractionation. It is not surprising that the terrestrial mass fractionation exponent derived from these data is between the kinetic and equilibrium values.

6.2. Δ^{17}O and the Dole Effect

If Earth's tropospheric O_2 were in isotopic equilibrium with the oceans, it would have a δ^{18}O value (relative to SMOW) close to zero. But O_2 in the lower atmosphere is enriched in $^{18}O/^{16}O$ by 23.5‰ relative to typical ocean waters ($\delta^{18}O$ = 23.5‰; Kroopnick and Craig, 1972). This enrichment in atmospheric oxygen δ^{18}O relative to ocean water is referred to as the Dole effect (Dole, 1935) and is the result of a steady state between production of O_2 by photosynthesis on land and in the oceans (δ^{18}O values of near +4 and 0‰, respectively; Farquhar et al., 1993) and the preferential uptake of ^{16}O relative to ^{18}O (and ^{17}O) during respiration (oxygen consumed during respiration has δ^{18}O on the order of 20‰ lower than the intake O_2; Epstein and Zeiri, 1988; Guy et al., 1993).

Recent studies suggest that δ^{17}O of tropospheric O_2 lies below the terrestrial fractionation line (TFL) on a plot of δ^{17}O against δ^{18}O by ~0.16 to 0.18‰ (i.e., $\Delta^{17}O \sim -0.16$ to −0.18; Fig. 2). Luz et al. (1999) attributed the depletion in ^{17}O to non-mass-dependent enrichments in ^{17}O and ^{18}O in the stratosphere. On this basis, these authors argue that because photosynthesis produces O_2 with Δ^{17}O values of zero (O_2 released during photosynthesis is similar to natural waters on the TFL), and respiration removes some of the atmospheric O_2 having the negative Δ^{17}O values, the magnitude of atmospheric oxygen Δ^{17}O can be used to estimate global biosphere production over time.

The basis for using Δ^{17}O as a tracer of global biologic activity is that biologically mediated mass-dependent fractionation of the three oxygen isotopes will produce compositions along a terrestrial mass fractionation curve common to the terrestrial oxygen reservoirs other than air (i.e., rock and water). However, fractionation of oxygen isotopes during respiration is a kinetic process, and if respired oxygen is compared with oxygen reservoirs dominated by equilibrium fractionation relative to standard mean ocean water, a negative Δ^{17}O is expected from purely mass-dependent fractionation.

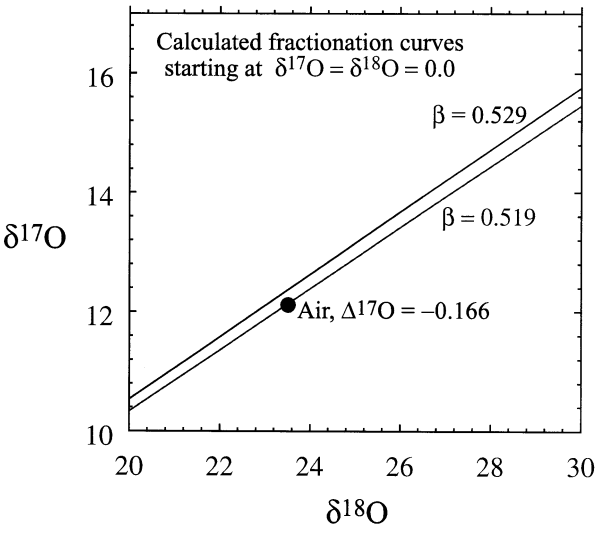

Fig. 2. Oxygen three-isotope plot showing that the difference in β values between a terrestrial fractionation curve ($\beta = 0.529$) and a kinetic respiration curve ($\beta = 0.519$) is sufficient to explain the Δ^{17}O of tropospheric O_2.

The values for β that characterize the relationship between δ^{17}O and δ^{18}O for terrestrial rocks and waters were measured recently with high precision by Miller et al. (1999) and Li and Meijer (1998), respectively. The value for rocks is 0.525 ± 0.001 (2σ) and the value for waters is 0.528 ± 0.002. Eqn. 15 predicts that β for oxygen exchanged under equilibrium conditions should be 0.5294. Matshuhisa et al. (1978) calculated partition function ratios for CO_2 and H_2O that give equilibrium βs for oxygen isotope exchange ranging from 0.5233 (T = 273.16K) to 0.5251 (T = 1000K). The partition function ratios provide equilibrium β values with fewer approximations than those used to derive the more general Eqn. 15. Rough agreement between β values obtained by high-precision measurements of rocks, Eqn. 15, and the more rigorous partition function calculations of Matsuhisa et al. (1978) suggests that oxygen isotope fractionation approaches equilibrium during most terrestrial rock-forming processes. This is not surprising because rocks acquire their isotopic compositions through processes that approach chemical equilibrium as well (e.g., igneous crystallization, carbonate precipitation in oceans).

The origin of the value for waters is less clear because of the influence of O-H reduced masses on the kinetic β. Eqn. 34 (equivalent to Eqn. 25 in this case where the m^*s in the latter are reduced masses) gives a kinetic β of 0.5286 for O-H bonds and 0.5270 for H-OH bonds. Both values are indistinguishable (with available data) from the equilibrium β. If the kinetics of reactions involving liquid water are dominated by O-H and/or H-OH stretching, then it is not possible to distinguish equilibrium from kinetic oxygen isotope fractionation in water (although it is possible to exclude the different rates of transport of water molecules as a controlling kinetic factor since Eqn. 25

and the molecular weights of water give a β of 0.5132, a value that is much lower than the measured value).

Regardless of their origins, the similar values for rock and water β values can be used to define a single TFL composed of these materials. For comparisons with studies that use a linear TFL, we note that linear regression (York, 1969) of the terrestrial curve defined by the origin and $\beta = 0.525$ over the range of $\delta^{18}O$ values typical of most rocks (+5 to +35‰) yields a straight line with a slope of 0.520 ± 0.002 (2σ) and a correlation coefficient of 1.0000 on a conventional oxygen three-isotope plot. The curvature of the fractionation law results in a linear slope less than β but does not perceptibly degrade the quality of the apparent linear fit.

Atmospheric O_2 should have a negative $\Delta^{17}O$ relative to the TFL because biologic fractionation should occur with β less than the near-equilibrium value of 0.525 that characterizes most rock. Eqn. 25 predicts that the exponent β for respiration should be closer to 0.515 for monatomic O or 0.5076 for molecular oxygen (for example, if we assume that fractionation of oxygen occurs by diffusion through the cytoplasmic membrane). Over the range in $\delta^{18}O$ commensurate with the Dole effect, fractionation curves with $\beta = 0.529$ (the equilibrium value estimated from Eqn. 15) and $\beta = 0.519$ are sufficiently divergent to explain the $\Delta^{17}O$ in air O_2 relative to the TFL (Fig. 2). For the measured TFL β of 0.525, a respiration β of 0.515 suffices to explain the 0.17 offset between rocks and tropospheric O_2.

It is straightforward to demonstrate that a steady-state negative $\Delta^{17}O$ (relative to rocks and waters) like that shown in Figure 2 will form rapidly in the atmosphere as a consequence of kinetic fractionation produced by respiration. The time scale for establishment of the steady state will be on the order of the O_2 turnover time of ~1 kyr (Bender et al., 1994). The steady-state isotopic composition can be simulated for illustration purposes by iteration on the equations

$$\delta\,^{18}O_{n+1} = \delta\,^{18}O_n + R_{photo}\,(\delta\,^{18}O_{H2O} + \Delta_{photo}) - R_{res}\,(\delta\,^{18}O_n + \Delta_{res}) \quad (39)$$

and

$$\delta\,^{17}O_{n+1} = (10^3 + \delta\,^{17}O^o)\left(\frac{10^3 + \delta\,^{18}O_{n+1}}{10^3 + \delta\,^{18}O^o}\right)^{\beta} - 10^3. \quad (40)$$

One finds that the steady state lies on a mixing line with a slope very nearly equal to β in Eqn. 40 (a consequence of the near linearity of the fractionation curves). In Eqn. 39 and 40, $\delta^{18}O_n$ and $\delta^{18}O_{n+1}$ are the isotopic compositions of O_2 in the n^{th} and $n^{th} + 1$ time steps, the superscript ^{o} refers to the initial values, R_{photo} and R_{res} are the rates of photosynthesis and respiration, $\delta^{18}O_{H2O}$ is the isotopic composition of ocean water, Δ_{photo} is the fractionation in $\delta^{18}O$ relative to ocean water associated with photosynthesis, and Δ_{res} is the fractionation relative to atmospheric O_2 associated with respiration. Starting with isotopic equilibrium between O_2 and ocean water, a steady state that matches present-day tropospheric $\Delta^{17}O$ and $\delta^{18}O$ in this simplified calculation is achieved with $R_{photo}/R_{res} \sim 1.75$, $\beta = 0.519$, $\Delta_{photo} = +2$, and $\Delta_{res} = -20$‰. The value for β will be prescribed by respiration since this process effects the largest change in the isotopic composition of O_2. The steady state depicted by convergence of Eqn. 39 and 40 is shown schematically in Figure 3.

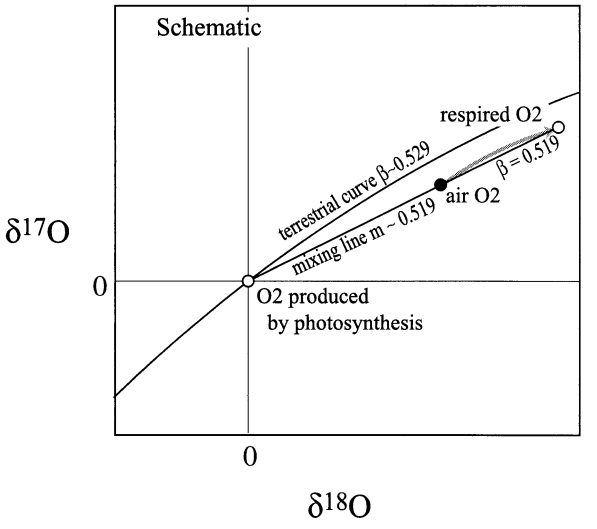

Fig. 3. Schematic illustration of the onset of a steady-state $\Delta^{17}O$ for tropospheric O_2 as a result of respiration. The grey arrow shows the relationship between free O_2 in the troposphere and respired O_2. The isotopic composition of tropospheric O_2 may be a consequence of a steady state, represented by the mixing line, between respired O_2 and O_2 produced by photosynthesis. After several cycles that begin with O_2 in equilibrium with ocean water (near 0‰), the O_2 evolves to a position on the mixing line between the isotopic compositions of O_2 produced by photosynthesis and that of respired O_2.

Respiration will keep atmospheric O_2 off the terrestrial line as long as the kinetic β is different from the β that characterizes the terrestrial curve (Fig. 3). Changes in $\Delta^{17}O$ are possible without a source of non-mass-dependent fractionation by altering the kinetic value for β, perhaps in response to changes in the proportions of biologic activities with different mass-dependent fractionation laws. For example, lowering β from 0.519 to 0.512 in these calculations doubles the steady-state $\Delta^{17}O$ relative to the terrestrial line from −0.141 to −0.305‰.

It is also possible to change $\Delta^{17}O$ of tropospheric O_2 by changing the relative rates of photosynthesis and respiration because this ratio of rates determines the steady-state $\Delta^{17}O$ and $\delta^{18}O$ of O_2. The terrarium experiments of Luz et al. (1999) may represent an extreme example of this behaviour. The data obtained from the experiments show a negative correlation between $\delta^{18}O$ and $\Delta^{17}O$ in response to changes in R_{photo}/R_{res}. Such a correlation is expected on the basis of mass-dependent fractionation alone; at lower $\delta^{18}O$, the value of $\Delta^{17}O$ becomes less negative (closer to zero) as the divergence between the equilibrium terrestrial curve and the mixing line between respired O_2 and photosynthetic O_2 becomes smaller (Fig. 3).

Although photolysis in the stratosphere is expected to contribute to a negative $\Delta^{17}O$ in atmospheric O_2 at some level (Luz et al., 1999), it is possible to interpret the $\Delta^{17}O$ of tropospheric O_2 as the natural consequence of kinetic fractionation during respiration using conservative differences between the β for respiration and that typical of rocks. For this reason it would seem premature to attribute the whole of the $\Delta^{17}O$ in tropospheric O_2 to mass-independent reactions in the stratosphere.

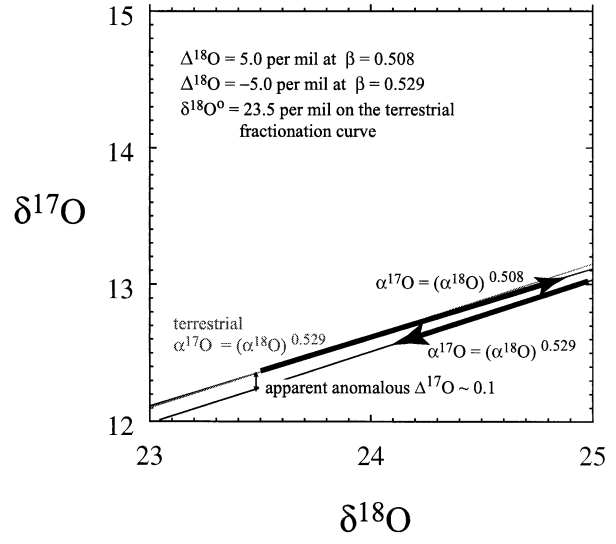

Fig. 4. Illustration of the shift in $\Delta^{17}O$ associated with 5‰ irreversible fractionation. The first portion of the path occurs with $\beta = 0.508$. The second segment occurs with $\beta = 0.529$. Each cycle will result in a decrease in $\Delta^{17}O$ of 0.1‰. Reversing the order of either of the shifts in $\delta^{18}O$ or the values of β results in an increase of 0.1‰ per cycle.

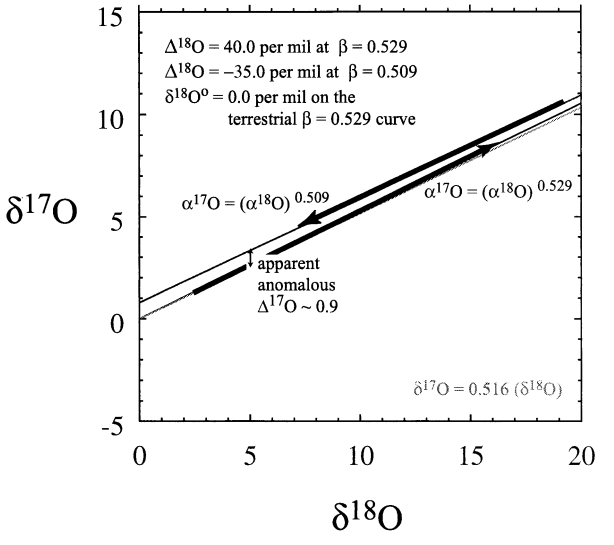

Fig. 5. Illustration of the shift in $\Delta^{17}O$ associated with 35 to 40‰ irreversible fractionation. Each cycle produces an increase in $\Delta^{17}O$ of 0.9‰.

6.3. Cyclical Kinetic Fractionation: A Mechanism for Small Differences in Meteorite $\Delta^{17}O$?

Without detailed knowledge of reaction pathways, assertions about departures from mass-dependent isotope fractionation at the sub-per mil level may be questioned. Where bonds are broken, reformed, and broken again, kinetic fractionation with different values for β may operate to drive products well off a given reference fractionation curve in three-isotope space. This is likely to occur because the kinetic steps are not generally reversible. Figure 4 shows the result of a fictive two-step reaction mechanism involving oxygen in which the first step results in a shift in $\delta^{18}O$ of +5‰ at a β of 0.508 and the second step results in a shift in $\delta^{18}O$ of −5‰ at a β of 0.529. The final product has a $\Delta^{17}O$ of 0.1‰ relative to the initial fractionation curve. A more extreme example is shown in Figure 5 in which the shifts in the two separate steps are on the order of 40‰ and the resulting $\Delta^{17}O$ is nearly 1‰. Such processes would produce non-zero intercepts on three-isotope plots that arise entirely from variations in β.

Farquhar et al. (1998) measured a positive $\Delta^{17}O$ in carbonate from SNC (Martian) meteorite ALH 84001 that exceeds the silicate $\Delta^{17}O$ in the meteorite by ~0.5‰. Karlsson et al. (1992) found that water extracted from SNC meteorites by pyrolysis has higher $\Delta^{17}O$ than silicates by a similar magnitude (0.4–0.9‰). Farquhar et al.(1998) offered the interpretation that these data are evidence for non-mass-dependent reactions driven by UV photolysis in the Martian atmosphere. However, it is also possible that numerous episodes of irreversible reactions, perhaps related to cycles of freezing and sublimation, caused the deviations in $\Delta^{17}O$ between the volatile components and silicates. If condensation and sublimation, for example, occurred with different values of β (freezing closer to equilibrium, sublimation closer to kinetic), then a steady-state disparity between $\Delta^{17}O$ in silicate rock in SNC meteorites and volatiles in the Martian atmosphere could occur after just a few freeze-thaw cycles (e.g., Figs. 4 and 5). The magnitude of $\Delta^{17}O$ resulting from freezing and thawing would depend on the span in β, the shift in $\delta^{18}O$ associated with the process and the relative rates of sublimation and condensation (by analogy with the Dole effect as described in section 6.2). Eiler et al. (2000) suggest that fractionation during freeze/thaw cycles may have been substantially greater than that in Figure 4, making it all the more likely that $\Delta^{17}O$ of volatile components in the Martian regolith differs from silicate rock $\Delta^{17}O$, at least in part as a result of mass-dependent fractionation.

7. SUMMARY AND CONCLUSIONS

The mass-dependent fractionation laws for three or more isotopes are different for equilibrium and kinetic processes. In both cases the fractionation law can be written as $\alpha_{2/1} = \alpha_{3/1}^{\beta}$. Equilibrium isotope exchange leads to $\beta \sim (1/m_1 - 1/m_2)/(1/m_1 - 1/m_3)$, where m_1, m_2, and m_3 represent the masses of the isotopes, whereas kinetic fractionation yields $\beta \sim \ln(M_1/M_2)/\ln(M_1/M_3)$, where M_1, M_2, and M_3 represent atomic, molecular, or reduced masses of the isotopologues in motion.

In practice, kinetic fractionation produces curves in three-isotope space that have shallower slopes than those produced by equilibrium exchange (e.g., where $\delta^{17}O$ or $\delta^{25}Mg$ is the ordinate and $\delta^{18}O$ or $\delta^{26}Mg$ is the abscissa). Experiments with Mg isotopes show that differences in isotope ratios of 3‰ per amu are sufficient to permit distinction between equilibrium and kinetic fractionation using current technologies.

The range in possible mass-dependent fractionation laws should be considered when seeking to identify sub-per mil deviations from mass dependency. Potentially important examples include the $\Delta^{17}O$ of tropospheric O_2 relative to terrestrial rocks and differences in $\Delta^{17}O$ between carbonate, hydroxyl, and anhydrous silicate in Martian meteorites.

Acknowledgments—This work represents the product of several technological innovations and experimental programs supported by various individuals. The contributions of Nick Belshaw (Oxford), Richard Ash (Oxford), and R. Keith O'Nions (Oxford) are especially appreciated. We also benefited from lengthy discussions with James Farquhar, Mark Thiemens, and Martin F. Miller. It was the careful experiments by Martin Miller and his colleagues that convinced us that the topic of mass-dependent fractionation could be explored further. E. D. Y. acknowledges support by a grant from PPARC (U.K.). A. G. was supported during this work by the EC through TMR "Marine Record of Continental Tectonics and Erosion" ERBFMXCT 960046.

Associate editor: R. Wieler

REFERENCES

Bender M., Sowers T., and Labeyrie L. (1994) The Dole effect and its variations during the last 130,000 years as measured in the Vostok ice core. *Global Biogeochem. Cy.* **8,** 363–376.

Bigeleisen J. (1949) The relative velocities of isotopic molecules. *J. Chem. Phys.* **17,** 675–678.

Bigeleisen J. (1955) Statistical mechanics of isotopic systems with small quantum corrections. I. General considerations and the rule of the geometric mean. *J. Chem. Phys.* **23,** 2264–2267.

Bigeleisen J. and Mayer M. G. (1947) Calculation of equilibrium constants for isotopic exchange reactions. *J. Chem. Phys.* **15,** 261–267.

Catanzaro E. J., Murphy T. J., Garner E. L., and Shields W. R. (1966) Absolute isotopic abundance ratios and atomic weight of magnesium. *J. Res. NBS A. Phys. Ch.* **70A,** 453–458.

Dole M. (1935) The relative atomic weight of oxygen in water and air. *J. Am. Chem. Soc.* **57,** 2731.

Eiler J. M., Kitchen N., and Rahn T. A. (2000) Experimental constraints on the stable isotope systematics of CO_2 ice/vapor systems and relevance to the study of Mars. *Geochim. Cosmochim. Acta* **64,** 733–746.

Epstein S. and Zeiri L. (1988) Oxygen and carbon isotopic compositions of gases respired by humans. *Proc. Natl. Acad. Sci.* **85,** 1727–1731.

Farquhar G. D., Lloyd J., Taylor J. A., Flanagan L., Syvertsen J. P., Hubick K. T., Wong S., and Ehleringer J. R. (1993) Vegetation effects on the isotope composition of oxygen in atmospheric CO_2. *Nature* **363,** 439–443.

Farquhar J., Thiemens M. H., and Jackson T. (1998) Atmosphere-surface interactions on Mars: $\Delta^{17}O$ measurements of carbonate from ALH 84001. *Science* **280,** 1580–1582.

Forst W. (1973) *Theory of Unimolecular Reactions.* Academic Press, New York.

Galy A., Young E. D., Ash R. D., and O'Nions R. K. (2000) The formation of chondrules at high gas pressures in the solar nebula. *Science* **290,** 1751–1753.

Galy A., Belshaw N. S., Halicz L., and O'Nions R. K. (2001) High-precision measurement of magnesium isotopes by multiple collector inductively coupled plasma mass spectrometry (MC-ICPMS). *Int. J. Mass Spectrom. Ion Proc.* **208,** 89–98.

Gao Y. Q. and Marcus R. A. (2001) Strange and unconventional isotope effects in ozone formation. *Science* **293,** 259–263.

Guy R. D., Fogel M. L., and Berry J. A. (1993) Photosynthetic fractionation of the stable isotopes of oxygen and carbon. *Plant Phys.* **101,** 37–47.

Hathorn B.C. and Marcus R.A. (1999) An intramolecular theory of the mass-independent isotope effect for ozone. I. *J. Chem. Phys.* **111,** 4087–4100.

Hathorn B. C. and Marcus R. A. (2000) An intramolecular theory of the mass-independent isotope effect for ozone. II. Numerical implementation at low pressures using a loose transition state. *J. Chem. Phys.* **113,** 9497–9509.

Hulston J. R. and Thode H. G. (1965) Variations in the S^{33}, S^{34}, and S^{36} contents of meteorites and their relation to chemical and nuclear effects. *J. Geophys. Res.* **70,** 3475–3484.

Karlsson H. R., Clayton R. N., Gibson E. K., and Mayeda T. K. (1992) Water in SNC meteorites: Evidence for a Martian hydrosphere. *Science* **255,** 1409–1411.

Li W. J. and Meijer H. A. J. (1998) The use of electrolysis for accurate $\delta^{17}O$ and $\delta^{18}O$ isotope measurements in water. *Isot. Environ. Healt. S.* **34,** 349–369.

Luz B., Barkan E., Bender M. L., Thiemens M. H., and Boering K. A. (1999) Triple-isotope composition of atmospheric oxygen as a tracer of biosphere productivity. *Nature* **400,** 547–550.

Marcus R. A. and Rice O. K. (1951) The kinetics of the recombination of methyl radicals and iodine atoms. *J. Phys. Colloid Chem.* **55,** 894–908.

Matsuhisa Y., Goldsmith J. R., and Clayton R. N. (1978) Mechanisms of hydrothermal crystallization of quartz at 250°C and 15 kbar. *Geochim. Cosmochim. Acta* **42,** 173–182.

Miller M. F., Franchi I. A., and Pillinger C. T. (1999) The mass-dependent oxygen isotope fractionation line: New measurements and the need for a reporting consensus. *Proc. Goldschmidt IX.* (abstract) pp. 7433.

Nagahara H. and Ozawa K. (1996) Evaporation of forsterite in H_2 gas. *Geochim. Cosmochim. Acta* **60,** 1445–1459.

Slater N. B. (1948) Aspects of a theory of unimolecular reaction rates. *Proc. Royal Soc. A.* **194,** 112–131.

Weston R. E. (1999) Anomalous or mass-independent isotope effects. *Chem. Rev.* **99,** 2115–2136.

Urey H. C. (1947) The thermodynamic properties of isotopic substances. *J. Chem. Soc. 562–581.*

York D. (1969) Least squares fitting of a straight line with correlated errors. *Earth Planet. Sci. Lett.* **5,** 320–324.

Zhu X. K., Guo Y., O'Nions R. K., Young E. D., and Ash R. D. (2001) Isotopic homogeneity of iron in the early solar nebula. *Nature* **412,** 311–313.